MOISTURE FLOW DISTRIBUTION IN STATOR BLADES OF STEAM TURBINES

Fernando Rueda-Martínez
Facultad de Ingeniería, Universidad Veracruzana campus Coatzacoalcos, México. frueda@uv.mx

Miguel Toledo-Velázquez
Laboratorio de Ingeniería Térmica e Hidráulica Aplicada, Instituto Politécnico Nacional, México. mtv49@yahoo.com

Aldo A. Rueda-Martínez
Laboratorio de Ingeniería Térmica e Hidráulica Aplicada, Instituto Politécnico Nacional, México. aldo_rueda2@hotmail.com

Quetzalcoatl C. Hernández-Escobedo
Facultad de Ingeniería, Universidad Veracruzana campus Coatzacoalcos, México. qhernandez@uv.mx

Francisco Espinosa-Arenal
Facultad de Ingeniería, Universidad Veracruzana campus Coatzacoalcos, México. franciespinosa@uv.mx

Abstract. *The velocity, enthalpy and pressure distribution of steam with moisture in a stator blade channel of the last stage of the low pressure section steam turbine of 30 MW is presented. The condensation conditions on the basis of the frictionless, two-dimensional, stationary, transonic and homogenous flow, in order to compute the droplet motion in a blade mesh configuration according to the finite volume method, are established. The distributions show inflections caused by presence of droplets localized in the 87% of curvature of the profile, in the outlet of throat on the suction surface, resulting in a variation of the expansion rate in the passage of blades. These droplets escaping from the stators blades impact the next crown rotor blades, developing the phenomenon of erosion.*

Keywords: *steam turbine, stator blades, droplets, condensation, moisture, erosion.*

1. INTRODUCTION

A calculation procedure at the outlet of a set of blades when the flow has a certain wet degree is presented. The main detail is to know the behavior and the influence in the geometry that this type of phenomenon can have in normal operation. Gyarmathy (1976) analyzed the problems in relation to the stream of saturated steam and described its characteristics and the behavior, developing the procedures for the calculation of the condensation process in steam turbines. Here, the drops distribution in a blade channel is obtained for a given parabolic distribution of velocity over the blade channel.

Moore (1976) developed a theoretical and experimental treatment for two-phase flow in steam turbines and compared this with measurements in cascades. Also, numerical and analytical techniques developed for flows in cascades of two-dimensionally. Similarly, also Bakhtar et. al. (1997, a, b) showed that large secondary droplets in saturated vapor stream are essentially responsible for the adverse effects of moisture. Young (1995) and White (2005) separately developed analytical and numerical models to study cascades with two-dimensional steam flow moisture in using a mesh type H in order to identify the streamlines through the cascade and interpolate the time variations of the pressure required for the calculation of moisture.

In blade cascades the flow of saturated steam is a nebula of droplets. Due to the accumulation that is formed on the stator blade, the water becomes to escape in form of large drops, generally toward the suction side of the following rotor blades, causing erosion damages as a consequence. This impact of droplets on the blade surfaces is essentially based in the range sizes affected by the forces of inertia. Therefore, these droplets cannot follow the path of the steam flow in the blade cascade. In power-producing steam turbines, up to 15% of the megawatt generating capacity can be lost due to erosion and buildup of blade deposits from the condensate, according to Plondke (2012). Erosion and reduction in efficiency are in relationship with the accumulation of the fine nebula drops on the blade profiles. Only the accumulation leads to the generation of large drops, which cause flow losses and erosion damage directly. The research described by Crane (2004) states that droplet smaller than 0.2μm is not deposited on the edges of the stator blades. Thereby, the observations show that is of practical importance an approximated calculation of the drop movement in a mesh configuration for a turbine, of the saturated steam and, in particular, of the accumulation of drops on the stator blades, if with the calculation procedure the fundamental characteristics of the velocity and pressure distribution are qualitative and quantitatively detectable, being the movement of water on the blade channel the distribution of velocity and local density of steam.

As condition for the calculation of the drop movement, first the velocity field of the steam in the blade cascade with a procedure appropriate for transonic condition in this work is developed. In order to calculate the compressible stream in blade cascades, the method of singularities was suitable. For calculating the transonic stream, the time step procedure is used. The generation of a stator blade mesh H in a Fortran code based in finite volume method permitted the calculation of the velocity and pressure distribution. The turbulent viscose stream in a turbine lattice like economic criteria is pointed out and can be seized only with an approaching model, whose inadequacy represents the neglect of all friction terms.

The present investigation reports that flow parameters showed inflections in the distributions localized in the throat zone of the stator blade passage, due to condensation before the exit of the cascade, indicating the presence of drops that can contribute to the development of erosion development in the leading edge of following rotor blade in the low pressure stage. This data is relevant to define the moisture presence in the stator blade channel and execute the necessary rules of prevention and maintenance in relation to the erosion problem that appears in these stages. This numerical solution is in accordance compared with theory and results of other authors.

2. TRANSONIC FLOW

In order to formulate the conservation laws a mesh configuration showed in Fig. 1 was made for this space. For a calculation of the transonic stream, the time step procedure was suitable. The constant k of ideal gas constant relationship for a medium of flow was accepted. The isentropic state change and the well-known gas dynamics basic relations are described.

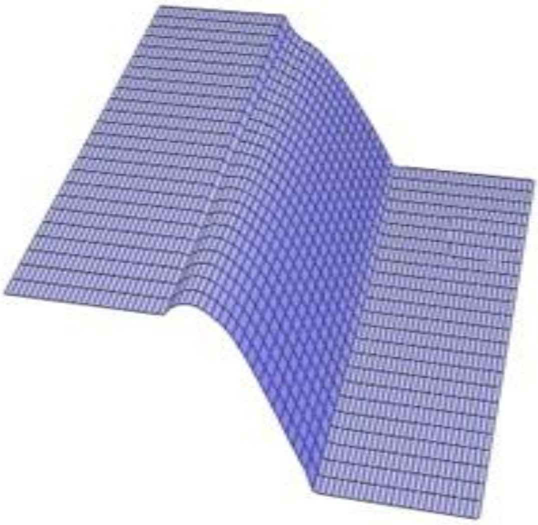

Figure 1: Designation of mesh for the zone of flow.

First, the law of change of state is accepted as polytropic

$$p_k = p_{in}\left(\frac{\rho_k}{\rho_{in}}\right)^n \tag{1}$$

$$\rho_S = \rho_{in}\left(\frac{p_S}{p_{in}}\right)^{\frac{1}{k}} \tag{2}$$

where index *in* refers to inlet flow condition in accordance with the point of mesh k and *S* refers to small quantities. A condition for the application of the Eq.(2) is that the mesh function and the leading edge crossing compression shocks are weak.

In the outline of the profile the condition is fulfilled if the velocity is tangential. Thus it was possible to interpolate the velocity, pressure and density of the fields, with regard to the size in the inlet and outlet linear plane.

In the closest section l_{min} the exit angle β_e can be written in the following form

$$\sin\beta_{e-is} = \frac{\dfrac{l_{\min}}{t}\left(\dfrac{k+1}{2}\right)^{-\frac{k+1}{2k-1}}}{M_{eis}\left(1+\dfrac{k-1}{2}M_{e-is}^2\right)^{-\frac{k+1}{2k-1}}} \tag{3}$$

Then, the theoretical exit angle $\beta_{e\text{-}is}$ of the mesh turbine results in the case of isentropic expansion on a given pressure side. The velocity, pressure and density fields were introduced as initial values for the iterative way. The pressure sizes p_{in} and p_e are well-known from the given state of flow. Also, in each case c_{in} and c_e are known with p_{in} and p_e from the Eq.(3) and the circulation is extended thereby over the whole element.

For the representation of the calculation procedure, the dimensionless formulation is introduced in addition of the following definition

$$P = \frac{p}{\rho_{in} a_{in}^2 M_{in}} \qquad \text{Pressure,} \tag{4}$$

$$\sigma = \frac{\rho}{\rho_{in}} \qquad \text{Density,} \tag{5}$$

$$U = \frac{\rho c_x}{\rho_{in} c_{in}} \qquad \text{Axial Velocity,} \tag{6}$$

$$V = \frac{\rho c_y}{\rho_{in} c_{in}} \qquad \text{Peripheral Velocity.} \tag{7}$$

On the basis of U, V, P and σ in function of τ, in a stream value of the temporal derivatives of all the points in the mesh, the Eq.(4) - (11) can be calculated

$$U_k(\tau+\Delta\tau) = U_k(\tau) + \frac{\partial U_k}{\partial_k}\Delta\tau \tag{8}$$

$$V_k(\tau+\Delta\tau) = V_k(\tau) + \frac{\partial V_k}{\partial\tau}\Delta\tau \tag{9}$$

$$\sigma_k(\tau+\Delta\tau) = \sigma_k(\tau) + \frac{\partial\sigma_k}{\partial\tau}\Delta\tau \tag{10}$$

$$P_k = P_{in}\sigma_k^n \tag{11}$$

and the magnitude U_k, V_k, σ_k at time $\tau+\Delta\tau$ and Eq.(11) are associated with P_k. The consequence of receiving the function values is the smooth, in order to avoid instabilities in the calculation, on which the calculation is around an interval $\Delta\tau$. The edges were treated simply representing the upper and lower delimitations of the profile blade range. Here the condition of periodicity was fulfilled.

The calculation of an unsteady drop movement in a zone of flow on blade profile proceeds from the differential equation

$$m_T \frac{dw}{dt} = \frac{1}{2}\rho\cdot w_{rel}^2\cdot c_w\cdot\pi\cdot r_T^2 \tag{12}$$

the drops with a spherical shape are due to the force by the surface tension. The drop radius is designated as r_{Tin} between the two streamline courses $\psi_{T,i}$ and $\psi_{T,i+1}$ in the levels i and $i+1$ in the mesh. For the calculation of drop courses the velocity field must be given by drops moving with the help of the Eq.(12). The amount of the relative velocity is

$$w_{rel} = \sqrt{(w_{Dx}-\dot{x})^2 + (w_{Dy}-\dot{y})^2} \tag{13}$$

The mid drop course in the steam flow between the courses $\psi_{T,i}$ and $\psi_{T,i+1}$ at inlet

$$\dot{m}_{Din,i} = \rho_{in}''(\bar{c}_{Din,i}\sin\alpha_{Din,i})[\Delta l_{in,i}\cos(\alpha_{Tin,i}-\alpha_{Din,i})]^2 \tag{14}$$

where $\vec{c}_{Din,i}$ is the velocity of the steam at inlet, $\alpha_{Din,i}$ is its direction selected identical to the steam streamlines in the mesh in the two surfaces parallel to the indicated level $\Delta l_{in,i}$ and $\Delta l_{in,i+1}$, and the term $\cos(\alpha_{Tin,i} - \alpha_{Din,i})$ of the steam quantity is referred to the drop course direction.

The droplet impact on the blade surface is essentially based in the range of particles with sizes affected by the forces of inertia. These droplets cannot follow the stream of the steam flow in the blade channel. These large droplets start to escape from the stator blades, generally toward the suction side of the following rotor blade, causing erosion problems. The drop distribution in the mesh outlet level was represented on the basis of a fundamental flow pattern in a blade channel. It mean that the drops before the mesh were distributed homogeneously.

A certain number of drops in the pressure side of the blade enter into contact with the profile, all of drops are closed strongly in a very thin layer on the profile surface and are finally concentrated finally along the flow in a narrow volume of the trailing edge, forming a water film. The remaining drops leave the mesh with a velocity that deviates in size and direction from the local steam velocity. In addition, they are distributed irregularly over the mesh.

An estimated initial distribution of the searched flow parameters *σ, P, U* and *V* was entered. With the advance of time the initial distribution and boundary conditions were kept constant and approximately iterated to the stationary solution. Then, the solution functions *σ, P, U* and *V* were converted into the material sizes *ρ, p* and *c*. This difference of the flow functions was successively under a barrier given by introduction of a constant specific total enthalpy for the entire computing area

$$\frac{k}{k-1} = \frac{h_{tot}}{p_S / \rho_S} \tag{15}$$

In addition, the first parameter ρ_{in} was selected in such a way that the given pressure P_{in} of Eq.(1) fulfills the turbine design. The control of the transonic flow calculations was accomplished by the comparing the inlet and outlet mass flows.

3. NUMERICAL RESULTS

The steam turbine analyzed in this study gives 30 MW of power and a stator blade passage is examined in the last stage. The pressure that reigns in the input of stator stage is 49 kPa, and the temperature is approximately 86°C. The humidity at the inlet of the stator blade was 8%.

The system of finite mesh was obtained in two dimensions from the flow channel of the stator blades. In order to this it was necessary to enter the coordinates of a steam turbine blade profile. Then, the profile coordinates were transformed with the angle that was selected through the suitable subroutine.

The geometry of the blade is given point by point and represented by polynomial factors. The outline computing mesh adapted for the blade cascades shown in the Fig. 1 was designed in order to calculate the expected gradients. The individual structure for the theoretical calculation of the flow with drops was compiled.

A small increase in pressure exists on the suction surface due to the fast condensation or presence or droplets moving in the flow, which is localized in the 87% of curvature of the profile. According to this, the condensation occurs before the exit of the cascade (in the throat) and the expansion rate can vary in the passage of blades (the pressure distribution decrease and increase in fast form in the throat zone). Due to this, the Mach number is less than the output if the vapor does not contain moisture. The results of the pressure calculated throughout the channel are indicated in the Fig. 2. The pressure distribution in the flow channel presents an inflection at 20% of the chord, which corresponds to the change of blade curvature.

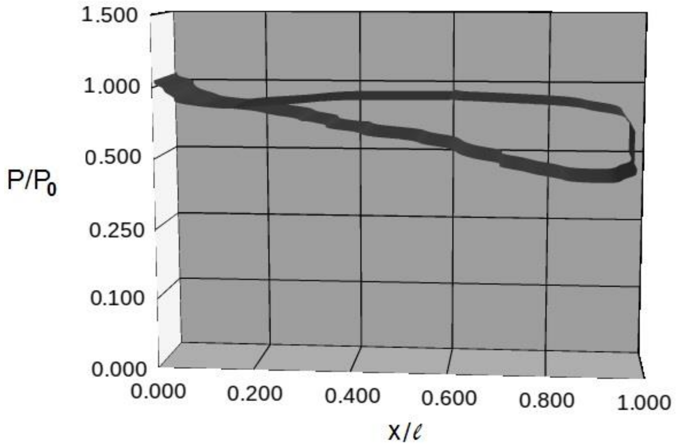

Figure 2: Graphic that shows the pressure values in the stator blade channel.

If Fig. 2 is compared with Fig. 3, it can be noted that the pressure in the proximity of the front stagnation point decreases with an increasing velocity. This behavior is due to condensation phenomenon that occurs near the surface pressure. There are later an accumulation of drops that reach the trailing edge of the blade. Another factor to be analyzed and which allows the above to be considered as valid is the behavior of the velocity in the flow channel, where the pressure decreases in the near side of the leading edge due to lower velocity of the steam flow and increases abruptly in the narrow part of the channel due to the increase in velocity.

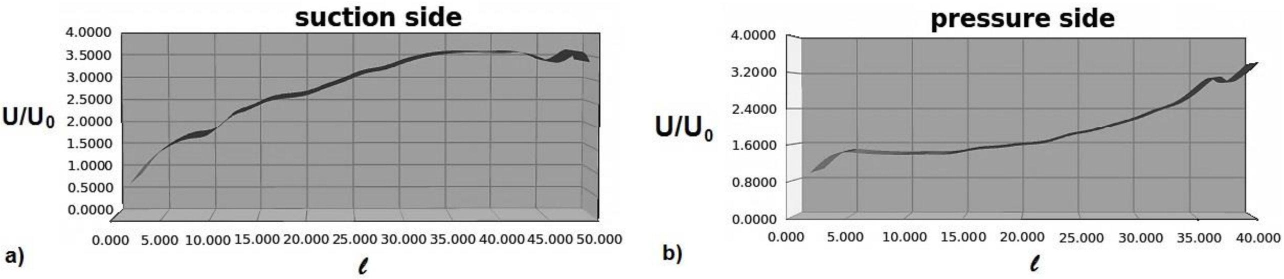

Figure 3: Graphic that show a) the behavior of the velocity distribution on the suction and b) pressure side in the stator blade channel.

In addition, it was guaranteed that M_{in} and β_e increase with the constantly increase of M_e, and that the continuity condition was thereby well satisfied. The calculations of the velocity distribution are indicated in Fig. 4. In both suction and pressure side graphics are shown an increasing value of the velocity of the flow over the surface, in according with Mach number in Fig. 2 and the pressure distribution in Fig. 3.

The quantitative results of the calculation represent the total enthalpy throughout the channel and are indicated in the Fig. 4. Here the pressure side in the superior part and the suction side in the inferior one are shown. The comparison between the calculated and isentropic total enthalpy shows that the arithmetic procedures in the leading edge have better agreement than in the trailing edge. The total enthalpy in the cascade is used as a convergence value for the stationary system. The lifted values of enthalpy in the pressure side indicate the presence of drops in 87% of the blade is of a more minor grade than in the suction side. The enthalpy shows that the droplets affect this zone when passing, interpreting this as an accumulation of the pressure side because they have been deposited in this part of blade, which affecting the flow in local form, due to the geometrical position of the blades. The values of enthalpy in the suction side indicate the presence of drops, since the phase change of steam to liquid is associated to less values of enthalpy.

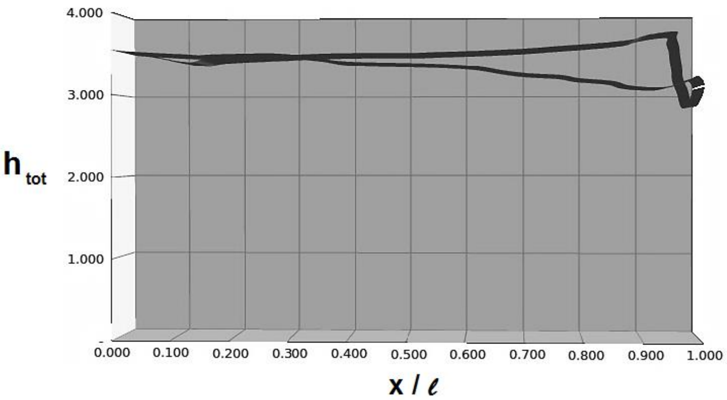

Figure 4: Graphic that shows the enthalpy calculation in the suction and pressure side in large *x/l* of the stator blade channel.

Figure 5 presents the calculation of impulse throughout the blade channel. In the inlet of the blade channel the impulse value of 2.9 is observed, and this impulse is going to be incremented due to the decrease of the pressure.

Figure 5a show the trailing edge of the pressure side of blade with a value of 7 kg/s·m^2, while in Fig. 5b this same value is found in 60% of the suction side but is observed that is surpassed from this point reaching a value of 8 kg/s·m^2 in the trailing edge. This is due to the geometrical disposition of the channel that converges with the throat in the pressure side on the suction side where the flow is guided by two solid surfaces. This causes an effect of acceleration on the flow, incrementing the impulse after the throat, controlled by a single surface, and then the flow approaches the next blade. Therefore, there is a change in the rate of expansion after the throat and a strong influence of suction surface in this region. The flow passes through the channel and first leaves from the pressure side in the throat zone. In this moment the impulse with a value of 7 kg/s·m2 is reached and the flow follows its way, increasing the impulse. It is noted that values of enthalpy dominate on the pressure side due to the flow, first leaving from this part of the blade and later from the suction side.

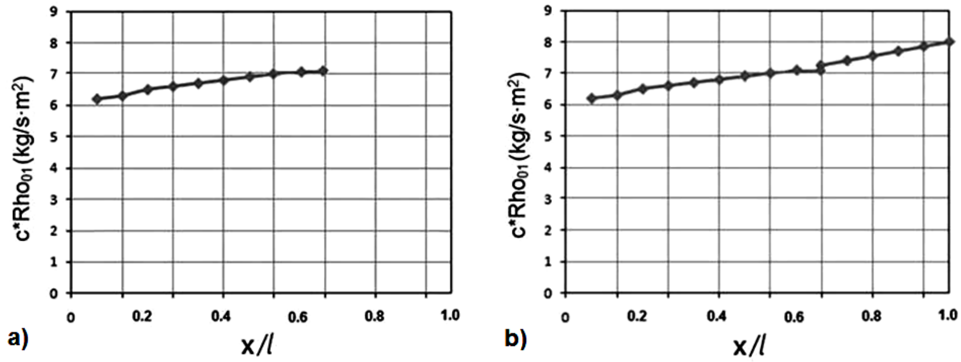

Figure 5: Graphic that shows the impulse in the stator blade channel on the a) pressure side and b) suction side.

Comparisons between calculated values and measurements made in the peripheral zone and the meridional section of pressure side, according to Gerber (2007), indicates that there is an accumulation of water in the section next to the trailing edge. It was also found that a common characteristic is that the increment of pressure in the moisture zone coincided with the change of curvature of the suction surface, as is shown in Fig. 6. This is partly because in the profiles studied the channel converges with the throat, where the flow is controlled by two solid surfaces. However, after the throat is controlled by a single surface and the flow approaches the next blade. Therefore, there is a sudden change in the rate of expansion after the throat and great influence of the suction surface in this region.

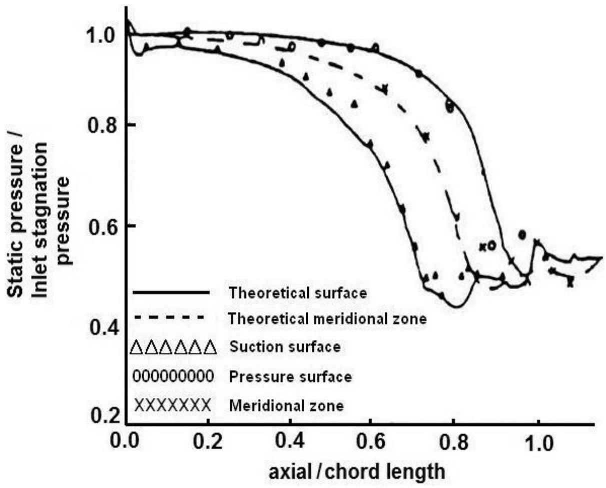

Figure 6: Comparison of the pressure distribution calculated from the measured pressure distribution in nozzles with wet steam flow (Gerber, 2007).

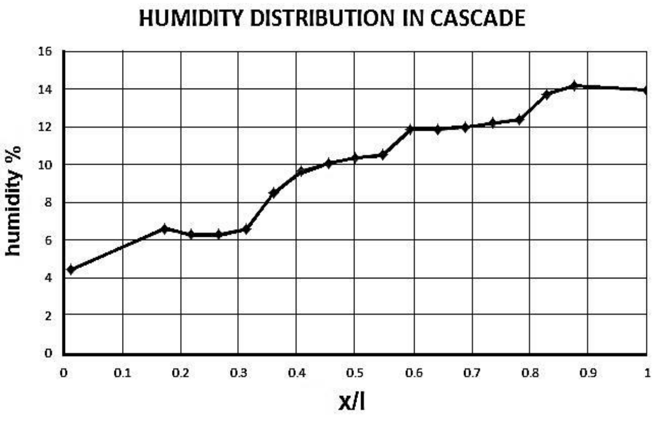

Figure 7: Percent moisture in the steam flowing in the channel that conform stator blades.

According to the results, Fig. 7 indicates substantial changes in the local distribution of droplets, the trend of which is their concentration in the trailing edge of pressure side of stator blades, forming a liquid film on the surface. This phenomenon is known as primary droplets accumulation. Comparing with other measurements of droplets, as is shown in Fig. 6, droplets larger than 0.2μm are approximately accumulated at 90% of the length on the pressure side of the stator blades forming a film that is separated from the trailing edge of the profile to become larger droplets, increasing the value of the moisture present in the channel as a result of condensation, which is greater in the output plane. In this study, a fraction of this percentage (0.46% calculated) is deposited on the surface of the stator blade. This moisture percentage is higher at the end of the cascade, indicating that the process of accumulation of drops in the stator blade is continuous, breaking the film that forms and the larger drops are those responsible for affecting the leading edge of the following rotor blade in the suction side.

Figures 8 and 9 confirm a distribution of water droplets in the flow channel formed by the turbine stator blades in two dimensions. Figure 8 indicates that the droplets whose diameter is about 0.2 μm do not significantly contribute to the accumulation of moisture on the stator blades, but a fraction exceeds 2% of humidity and belongs to droplets of 1-2 μm on the pressure surface of the stator blade. The presence of droplets on the suction surface is less without significant effects on the formation of subsequent larger droplets. Figure 9 shows a comparison between theoretical and experimental radii calculated by Gerber (2007). The theoretical values for the drop sizes show the same trend for a given growth rate (the flow channel A has the highest rate of expansion) whereas the experimental values vary in lower levels; but they are within the expected range.

There is a point in each studied flow channel in which the droplets stop growing and maintain their size; they therefore do not exceed 0.2 μm, indicating that these drops are not deposited on the surface of the corresponding stator blade. According to this, the approaches in predicting the water droplet sizes distribution to the axial direction, in Fig. 8 is obtained.

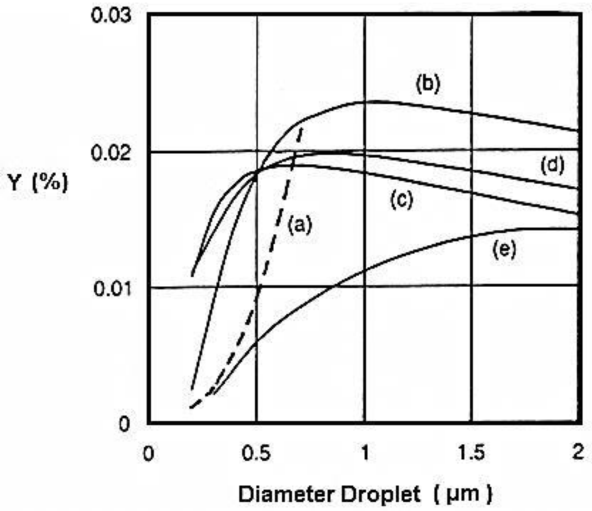

Figure 8: Accumulation of droplets in turbine blade low pressure on a) pressure surface of stator blade in the last stage, meridional section, b) pressure surface of stator blade in the last stage, meridional section, c) suction surface of stator blade in the last stage, tip, d) suction surface of rotor blade in the last stage, meridional section, and e) pressure surface of stator blade in the last stage, meridional section (Crane, 2004).

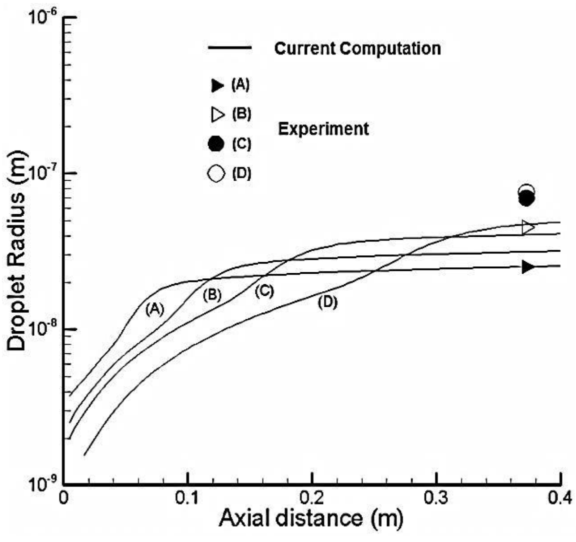

Figure 9: Comparison of the average radius calculation for different drops against values measured in different flow channels of stator blades (Crane, 2004).

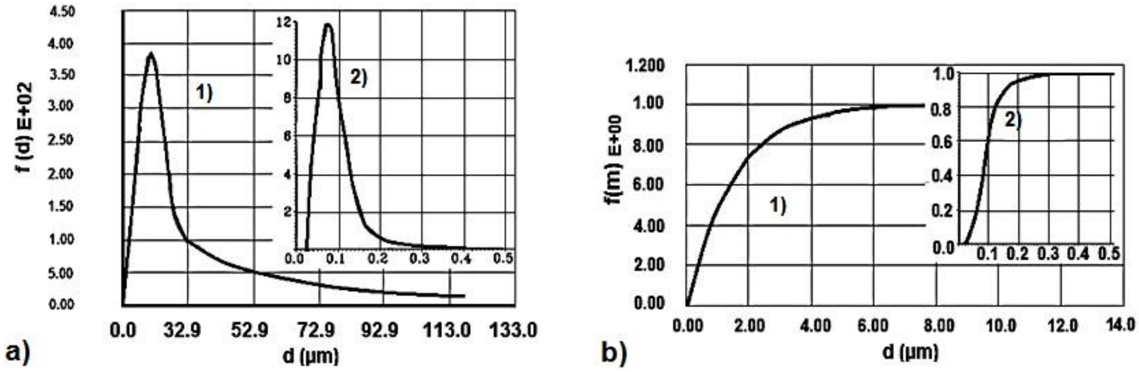

Figure 10: a) Graphic of probability distribution function of droplet sizes for 1) 30 MW low pressure steam turbine and 2) occurring in the 200 MW low pressure steam turbine, b) graphic of probability distribution function of mass droplets smaller for 1) 30 MW low pressure steam turbine and 2) occurring in the 200 MW low pressure steam turbine.

It can be seen in the case of study in Fig. 10(a) in comparison with Fig. 10(b) conducted by Petr (2000) about sizes of the droplets in the bell curve symmetric with the average diameter and the maximum at that point, showing the probability density function relative to diameter of droplets that appear in a wide range of expansion rates, covering the high values within the blade passage and almost zero values between the blade rows. Figures 10(a) and 10(b) demonstrate the fraction of mass droplets smaller in the distribution and this function becomes stable before reaching the average diameter. Therefore, it yields a broader droplet size spectra in this comparison, both for the stator blade case and the rotor ones for different powers. However, considering the experimental uncertainty in the measurements of droplet size, comparisons are in qualitative agreement.

4. CONCLUSIONS

The distributions show inflections in connection with the highest percentage of moisture in the output of the throat of the channel, due to the change of the curvature radius of the suction surface. The moisture percentage obtained increased at the output of the cascade, making the presence of drops in the stator blade continuous. These drops can contribute to develop a liquid film and generate larger drops that affect with the mechanical erosion of impact of droplets in the leading edge of following rotor blades on the suction side. Due to this moisture, the concentration of the properties of fluid, differ from those cascades of blades that work with superheated vapor. This fact defines the amount of moisture that remains in the channel and it is possible to carry out the necessary actions of prevention and maintenance with respect to the erosion problem that has originated for this reason.

5. REFERENCES

Bakhtar F., Mahpeykar M. R., 1997; "On the Performance of a Cascade of Turbine Rotor Tip Section Blading in Wet Steam. Part 3: Theoretical Treatment"; Proceedings of the Institute of Mechanical Engineers; Vol. 211, Part C; pp. 195-209.

Bakhtar F., Mashmoushy H., Jadayel O. C., 1997; "On the Performance of a Cascade of Turbine Rotor Tip Section Blading in Wet Steam. Part 2: Surface Pressure Distributions"; Proceedings of the Institute of Mechanical Engineers; Vol. 211, Part C; pp. 531-540.

Crane I. R., 2004; Droplet Deposition in Steam Turbines; Mechanical Engineering Science; Vol. 218. Part C; pp. 860.

Gerber A. G., 2007; Representing Polydispersed Droplet Behavior in Nucleating Steam Flow; Editorial ASME. Vol. 129; pp. 1406.

Gyarmathy G., 1976; Two Phase Steam Flow in Turbines and Separators, Theory, Instrumentation, Engineering. Condensing in Flowing Steam; Editorial McGraw-Hill Company; pp. 127.

Moore M. J., 1976; Gas Dynamics of Wet Steam and Energy Losses in Wet-Steam Turbines; Editorial Mcgraw-Hill Company; pp. 91; 1976.

Plondke A. C., 2012; Master Thesis: Droplet Characterization in the Wake of Steam Turbine Cascades; University of Tennessee Space Institute; pp. 2.

Petr V., Kolovratnik M., 2000; Modelling of the Droplet Size Distribution in a Low Pressure Steam Turbine; Journal of Power and Energy, Proceedings of the Institution of Mechanical Engineers: Part A, March 1, 214: 145-152.

White J. A., 2005; Theoretical Treatments of Two-Dimensional Two-Phase Flows of Steam and Comparison with Cascade Measurements; Mechanical Engineering Science; Vol. 219, Part. A; pp. 1335.

Young J. B., 1995; Wet-Steam Research at Cambridge 1980-1995; Editorial EPRI Workshop; pp. 6-10.

6. RESPONSIBILITY NOTICE

The authors are the only responsible for the printed material included in this paper.